Food Chemistry: Molecular Sciences 12 (2026) 100421

Contents lists available at ScienceDirect

Food Chemistry: Molecular Sciences

journal homepage: www.sciencedirect.com/journal/food-chemistry-molecular-sciences

Proteomic responses to the effect of coprophagy prevention on meat quality in New Zealand white rabbits

Hui He [a,b,1], Zhitong Wang [a,1], Zhichao Li [a], Mengke Ni [a], Mengjuan Chen [a], Chaohui Guo [a], Yaping Wang [a], Hanfang Cai [a], Ming Li [a,*], Huifen Xu [a,*]

[a] College of Animal Science and Technology, Henan Agricultural University, Zhengzhou 450046, PR China
[b] Agricultural and Rural Comprehensive Service Center of Qiaomu Township, Chizhou 242806, Anhui, PR China

ARTICLE INFO

Keywords:
Coprophagy prevention
Growth performance
Fatty acids
Oxidative phosphorylation
Proteomics

ABSTRACT

Coprophagy is an innate behavior of rabbits, and rabbit meat is favored by consumers for its distinctive nutritional characteristics. However, the relationship between coprophagy and meat quality in rabbits remains unclear. Therefore, this study investigated the effects of coprophagy prevention on growth performance and meat quality using a coprophagy-prevention model. The results showed that coprophagy prevention reduced growth performance and several meat quality parameters while increasing muscle fiber density. In addition, coprophagy prevention altered the nutritional composition of skeletal muscle by reducing unsaturated fatty acids (UFAs) and essential amino acids (EAAs), while increasing total lipid content and the proportion of saturated fatty acids (SFAs). Tandem mass tag (TMT)-based quantitative proteomic analysis identified 267 differentially expressed proteins (DEPs) in skeletal muscle following coprophagy prevention, which were mainly enriched in pathways related to muscle development, energy metabolism, fatty acid transport, and lipid metabolism. Further analyses suggested that alterations in lipid deposition and fatty acid composition may be associated with changes in mitochondrial oxidative phosphorylation and ATP production; however, these mechanistic relationships require further validation. Although several cognition-related pathways and reduced serum dopamine (DA) and 5-hydroxytryptamine (5-HT) levels were observed, the functional significance of these findings remains unclear due to the lack of behavioural assessments. Overall, the present study suggests that coprophagy prevention is associated with impaired growth performance and altered meat quality in rabbits. These findings provide preliminary insights into the potential metabolic changes associated with coprophagy prevention and highlight the biological importance of coprophagy in rabbit production.

1. Introduction

In recent years, rabbit meat has attracted increasing consumer interest due to its desirable sensory qualities and favorable nutritional profile. It is characterized by a high content of polyunsaturated fatty acids (PUFAs), high-quality protein, and essential amino acids (EAAs), while containing relatively low levels of fat and cholesterol, making it an excellent source of animal protein (Li et al., 2018). However, over the long course of natural selection and evolution, rabbits have developed and maintained the behavior of ingesting soft feces as an adaptation to adverse living conditions (Soave & Brand, 1991; Thacker & Brandt, 1955). Due to their digestive physiology and limited food availability, many small herbivores, including rabbits, have expanded the size of their foregut or hindgut regions to facilitate the fermentation of indigestible dietary fibers and engaged in coprophagy to meet their nutritional requirements (Ebino, 1993).

Studies have shown that coprophagy enables rabbits to reabsorb nutrients, including EAAs, short-chain fatty acids (SCFAs), and trace elements, and to replenish cecal microbiota, thereby maintaining gut microbial homeostasis (Bo et al., 2020; Combes et al., 2014; Hu et al., 2021; Savage, 1986). Notably, butyrate can enhance the integrity of the mucus layer and improve intestinal barrier function by upregulating MUC2 expression and promoting the differentiation and secretion of goblet cells (Burger-van Paassen et al., 2009; Hays et al., 2024). A healthy intestinal barrier facilitates the absorption of nutrients, electrolytes, and water, while effectively preventing the transepithelial

* Corresponding authors.
E-mail addresses: liming@henau.edu.cn (M. Li), huifen221@126.com (H. Xu).
[1] These authors have contributed equally to this work and share first authorship.

https://doi.org/10.1016/j.fochms.2026.100421
Received 20 November 2025; Received in revised form 21 May 2026; Accepted 22 May 2026
Available online 22 May 2026

transport of toxins and antigens (Stoeva et al., 2021). Therefore, SCFAs play a crucial regulatory role in maintaining intestinal health as well as the normal growth and development of livestock. Furthermore, accumulating evidence indicates that both dietary amino acids and intestinal microbiota play important roles in regulating meat quality, including its nutritional value and sensory attributes (Koyun et al., 2022; Liao et al., 2025). In our recent studies, we established a coprophagy-prevention model in rabbits using collars to inhibit the behavior. The results showed that preventing coprophagy altered gut microbiota composition, reduced short-chain fatty acid levels in cecal contents, and affected hepatic lipid metabolism (Li, Feng, & He, 2020; Wang et al., 2019; Wang et al., 2023).

Based on these findings, we hypothesize that preventing coprophagy may inhibit the reabsorption of EEAs and SCFAs, thereby affecting growth performance and meat quality in rabbits. Therefore, this study aimed to investigate the effects of coprophagy prevention on meat quality and nutritional composition using an established coprophagy-prevention model, and to identify key protein pathways and potential regulatory mechanisms associated with this behavior through proteomic profiling. Collectively, this study provides a theoretical foundation for elucidating the potential mechanisms by which coprophagy influences meat quality.

2. Materials and methods

2.1. Animal ethics

All procedures involving rabbits in this study was designed and performed in strict accordance with the guidelines of the Institutional Animal Care and Use Committee of College of Animal Science and Technology of Henan Agricultural University, China (No: 11–0085).

2.2. Animals

Eighteen healthy male New Zealand white rabbits, 46 days old, with similar body weight (1.79 ± 0.21 kg, mean ± SD) were provided by Mengfei Rabbit Breeding Co., Ltd. (Zhengzhou, China). After being assigned to groups, the rabbits were housed individually in a wire cage (50 × 40 × 40 cm^3). During the experiments, rabbits were housed in animal rooms at 24 ± 1 °C, with a photoperiod of 16Light: 8Dark. Rabbits had ad libitum access to water and granular diets. The composition and nutritional components of the diets are shown in Table S1. The pretrial and experimental periods were 7 and 42 days, respectively.

2.3. Animal treatment and sampling

Rabbits were assigned into three groups ($n = 6$): the control group (CON), the sham-coprophagy prevention group (SCP), and the coprophagy prevention group (CP). As shown in Fig. 1A, rabbits in the CON group were fed normally without a collar, rabbits in the sham-coprophagy prevention group were fitted with a narrow collar (5.0 cm in width) that did not prevent them from coprophagy, and rabbits in the coprophagy prevention group were fitted with an 8.5 cm width collar that prevented them from eating their own soft feces. Feed intake was recorded daily, and body weight (BW) was measured once a week. After the experimental period, rabbits were deprived of food and water for 24 h before slaughter. Subsequently, rabbits were euthanized under deep anesthesia with an overdose of isoflurane (Abbott, Chicago, IL, USA), followed by exsanguination via the carotid artery to collect tissue samples. Slaughter order followed a fixed cyclic sequence (CON–SCP–CP; two animals per group per cycle) rather than full randomisation. While this ensured temporal interspersion of treatments, it does not eliminate potential systematic order effects associated with processing time. The leg muscles of rabbits were collected for meat performance detection and tandem mass tag (TMT) proteomic analysis.

2.4. pH and meat color of the rabbit hind leg muscle

The pH of the biceps femoris was measured 45 min and 24 h after slaughter (six biological replicates, $n = 6$). After slaughter, the biceps femoris was stored at 4 °C for 24 h. The measurement was carried out by directly inserting the electrode of a pH meter (Testo206-Ph3, Testo SE & Co. KGaA, Lenzkirch, Germany). The pH meter was calibrated with pH 4.00 and 6.86 buffers at 25 °C (ambient temperature). The electrode was inserted sufficiently into the sample to ensure stable measurement. Each sample was tested three times, and the final result was calculated as the average.

The biceps femoris samples (six biological replicates, $n = 6$) were allowed to bloom at ambient temperature (25 °C) for 45 min. The color of the meat was recorded 45 min and 24 h after slaughter using a colorimeter (Opto-Star, Matthäus GmbH, Eckelsheim, Germany) based on the CIE LAB trichromatic system, which includes L^* (lightness), a^* (redness), and b^* (yellowness). Before measurement, the colorimeter was calibrated with an illuminant of D65, an observer angle of 10°, and an aperture size of 5.0 mm. The average color values were obtained by measuring the same muscle sample three times at three different locations.

2.5. Measurement of cooking loss percentage

Cooking loss was measured in accordance with a previous study (Kokoszyński et al., 2019). Biceps femoris samples (six biological replicates, $n = 6$) were cut parallel to the muscle fiber direction into pieces measuring approximately 4 cm × 2 cm × 1 cm and weighed precisely (8.5 ± 0.5 g). Each sample was placed in a resealable plastic bag and heated in a water bath at 85 °C until the internal temperature reached 70 °C. The liquid released during heating was then discarded, the bag was resealed, and the sample was rinsed under running water to cool. After cooling, the surface moisture was gently removed with a paper towel, and the sample was weighed again. Cooking loss was calculated as the difference between the weights of the raw and heat-treated samples and expressed as a percentage of the initial weight. All samples were processed in a single cooking batch.

2.6. Measurement of drip loss percentage

Biceps femoris samples (six biological replicates, $n = 6$) were trimmed into a particular shape (4 cm × 2 cm × 1 cm) and weighed accurately (8.5 ± 0.5 g). Then, the samples were suspended in a plastic box. After being stored at 4 °C for 24 h, the samples were dried with filter paper and weighed again. The drip loss was calculated as the difference between the weights before and after chilling and presented as a percentage of the initial weight.

2.7. Measurement of shear force

Biceps femoris samples (six biological replicates, $n = 6$) were prepared and cooked as previously described by Hopkins and Thompson (Hopkins & Thompson, 2001). Cut three samples with a cross-sectional area of 1 cm^2 along the direction of the muscle fibers for testing. Shear force was measured by a meat tenderness tester (C-LM3B, TENOVO, Beijing, China). The peak force was recorded as the shear force when cutting the rabbit leg samples. The mean value obtained from three repeated measurements was used as the muscle shear force value for each individual.

2.8. Chemical composition of the rabbit hind-leg muscle

The contents of moisture and ash in the biceps femoris of rabbits were measured in accordance with a previous study (Jin et al., 2021). Briefly, muscle samples (six biological replicates, $n = 6$; 20 ± 0.1 g each) were placed into a weighing bottle and dried to a constant weight in an

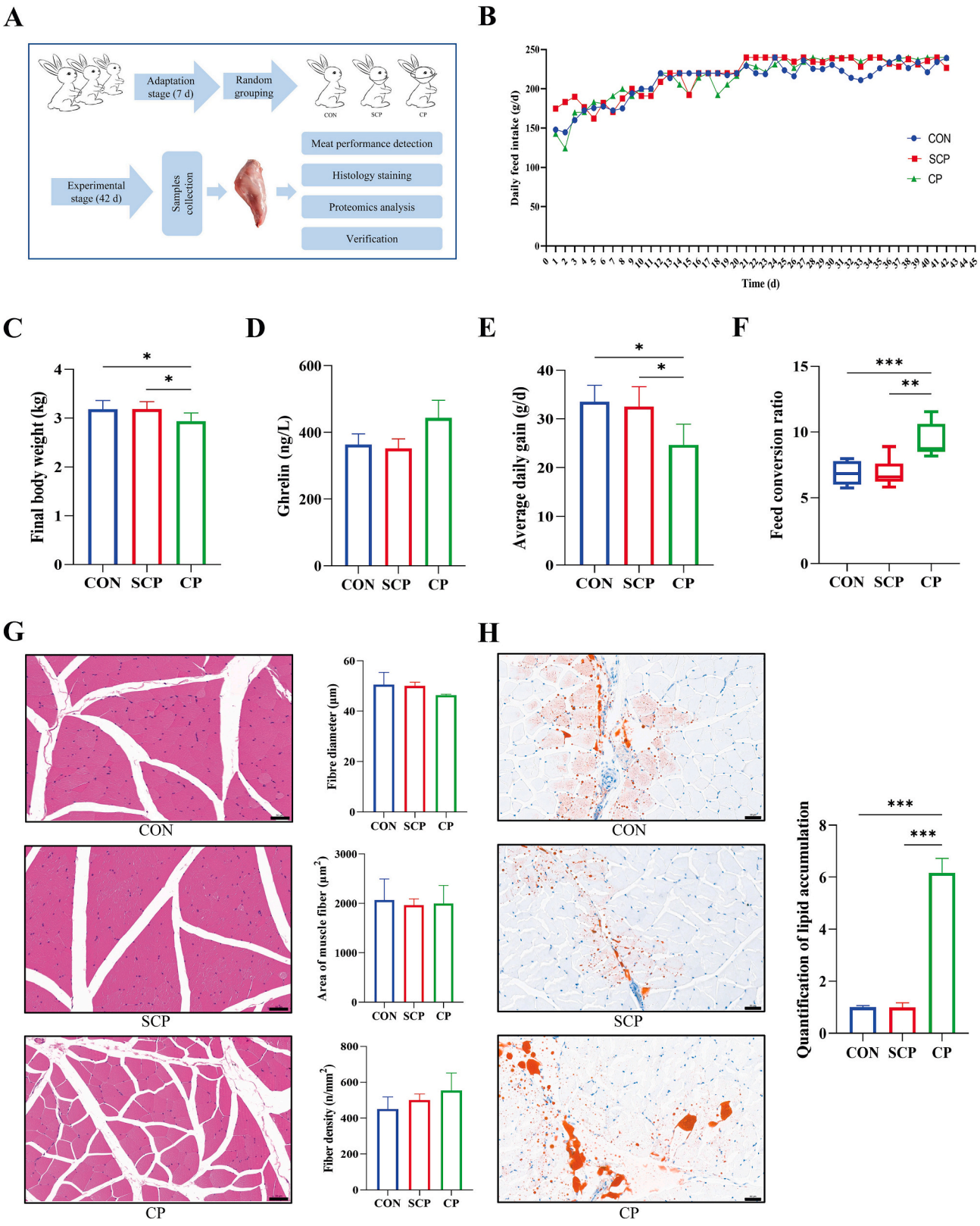

Fig. 1. Effects of CP on growth performance in rabbits. (A) Schematic diagram showing the study design. The daily food intake (B), final body weight (C), serum ghrelin level (D), average daily gain (ADG) (E) and feed conversion ratio (FCR) (F) of the CON, SCP and CP groups. Hematoxylin and eosin staining and quantitative index of muscle fiber (G) and oil red O staining of lipid droplet secretion and accumulation (H) in rabbit hind-leg muscle (scale bar = 50 μm). CON = control, SCP = sham-coprophagy prevention, CP = coprophagy prevention; $n = 6$. Values are presented as mean ± SEM. The asterisks symbol indicates significant differences (*$0.01 < p \leq 0.05$, **$0.001 < p \leq 0.01$, ***$p \leq 0.001$). (For interpretation of the references to color in this figure legend, the reader is referred to the web version of this article.)

oven maintained at 105 °C to obtain total solids. The total protein and triglyceride contents were measured by using the total protein (A045–2-2, Jiancheng, Nanjing, China) and triglyceride assay kits (A110–1-1, Jiancheng, Nanjing, China), respectively.

2.9. Determination of fatty acid and amino acid contents

The composition and content of fatty acids (six biological replicates, n = 6) of rabbit hind-leg muscle were measured according to the previous study (Souza Vilela et al., 2021). Briefly, meat samples (0.2 g) were ground with liquid nitrogen and transferred into 15 mL centrifuge tubes, 2.0 mL of triglyceride undecanoate solution (dissolved in methanol) was added as an internal standard (0.02 mg/mL), followed by the addition of 2 mL concentrated sulfuric acid/methanol solution (5%) and 10 μL BHT methanol solution (4 mg/mL), then the tubes were mixed with a vortex mixer for 1 min. Then the tubes were kept at 90 °C for 30 min, and cooled to room temperature. 2 mL normal hexane and 2 mL saturated sodium chloride solution were added to the mixture and mixed for 1 min. After standing for 15 min, the supernatant was collected and subjected to fatty acid composition analysis by using gas chromatography (Agilent 6890 N, Agilent Technologies, Santa Clara, CA, USA). The capillary column was 30 m × 0.25 mm, with a film thickness of 0.25 μm. (SGE Analytical Science, Ringwood, Victoria, Australia). The inlet temperature was 270 °C, it's pressure was 107.8 kPa, nitrogen was used as the carrier gas, the split ratio was 100:1, and the injection volume was 1.0 μL. The initial oven temperature was set to 100 °C and held for 13 min; increased at 10 °C per min to 180 °C, held for 6 min; increased at 1.0 °C per min to 200 °C, held for 20 min; then increased at 4 °C per min up to 230 °C where this temperature was maintained for 10.5 min. FID temperature was 280 °C with instrument air at 350 mL per min, and nitrogen make-up gas at 30 mL per min. Prior to sample analysis, the chromatographic peaks in the mixed fatty acid methyl ester standard solution were identified. The samples were then analyzed, and quantification was performed based on the peak areas.

Amino acid (six biological replicates, $n = 6$) composition and content of rabbit hind leg muscle were measured with the L-8900 automatic amino acid analyzer (HITACHI, Tokyo, Japan) as described by Huo et al. (2021). In short, 1.0 g muscle sample was ground into mud and then moved into the glass bottle, followed by addition of 10 mL HCl (6 mol/L). Following filling with nitrogen, the mixture was hydrolyzed at 110 °C for 24 h. Ultimately, the hydrolysate was transferred into a 50 mL volumetric flask and diluted with ultrapure water in a calibrated tube. The solution was filtered into the autosampler vial using a 0.22 μm membrane filter. Inject equal volumes of the mixed amino acid standard working solution (100 nmol/mL) and the sample solution into the amino acid analyzer, and determine the concentration of amino acids in the sample solution by calculating the peak area using the external standard method.

2.10. Histological staining

The hematoxylin and eosin (HE) staining of the hind leg muscle was performed in accordance with a previously reported method (Zhu et al., 2017) by the Servicebio Co., Ltd. (Wuhan, China). Visualization was carried out using an optical microscope (Eclipse Ci-L, Nikon, Tokyo, Japan). The biceps femoris (six biological replicates, n = 6) was fixed with paraformaldehyde, embedded in paraffin, and then cut into 5 μm sections. Oil Red O staining was performed on these sections under a Nikon optical microscope (Eclipse E100, Nikon, Tokyo, Japan) to measure the accumulation of lipid droplets. Use grid sampling to select fields of view for each slice; select four fields of view from each slice and calculate the average as the final result. The Image-Pro Plus 6.0 software (Media Cybernetics, Houston, TX, USA) was used for analysis.

2.11. Protein extraction, digestion, and TMT labeling

Based on the criterion of proximity to the group mean, four representative samples were selected from each group for proteomic analysis. All meat samples were homogenized in lysis buffer (4% SDS, 1 mM DTT, 150 mM Tris-HCl pH 8.0, protease inhibitor). After protein extraction, the bicinchoninic acid (BCA) protein assay reagent (P0010S, Beyotime, Shanghai, China) was used to determine the protein content. Then, the samples were stored at −80 °C until use. Protein digestion was performed in accordance with the FASP procedure described by Wiśniewski et al. (2009); the resulting peptide mixture was labeled using the TMTpro™ 16plex Label Reagent Set (Thermo Fisher Scientific, Waltham, MA, USA) according to the manufacturer's instructions (Applied Biosystems). For labeling, each TMT reagent was dissolved in 70 μL ethanol, and then added to the peptide mixture. Samples were labeled as (CON)-126, 127 N, 127C, 128 N, (CP)-128C, 131 N, 131C, 132 N, (SCP)-132C, 133 N, 133C, and 134, multiplexed, and vacuum-dried.

2.12. Peptide fractionation with strong cation exchange (SCX) chromatography

TMT-labeled peptides were fractionated by SCX chromatography using the AKTA Purifier system (GE Healthcare Life Sciences, Marlborough, MA, USA). The dried peptide mixture was reconstituted and acidified with 2 mL buffer A (10 mM KH2PO4 in 25% ACN, pH 3.0). Then, it was loaded onto the PolySULFOETHYL 4.6 × 100 mm column (5 μm, 200 Å, PolyLC Inc., Columbia, MD, USA). The elution process and fraction collection were carried out according to the previous study (Zhao et al., 2015). The liquid chromatography gradient program was set as follows: solvent B (10 mM KH2PO4 and 500 mM KCl in 25%ACN, pH 3.0) was linearly increased from 0% to 10% over 0–25 min, from 10% to 20% over 25–32 min, from 20% to 45% over 32–42 min, and from 45% to 100% over 42–47 min. Solvent B was then maintained at 100% from 47 to 60 min. After 60 min, solvent B was returned to 0% for column re-equilibration. Elution was monitored by measuring absorbance at 214 nm, and fractions were collected at 1-min intervals. The collected fractions were lyophilized and subsequently desalted using C_{18} cartridges. All samples were stored at −80 °C until LC-MS/MS analysis.

2.13. Liquid chromatography (LC)–electrospray ionization (ESI) tandem MS (MS/MS) analysis by fusion orbitrap

The specific assay method and procedure are the same as those in a previous study (Zhou et al., 2018). Each fractionated sample was separated using a nano-flow HPLC system (Easy-nLC, Thermo Fisher Scientific, Waltham, MA, USA). The mobile phases consisted of solvent A (0.1% formic acid in water) and solvent B (0.1% formic acid in acetonitrile–water, containing 84% acetonitrile). The analytical column was equilibrated with 95% solvent A prior to sample loading. Samples were injected by an autosampler onto a trap column (Thermo Scientific EASY Column, 100 μm × 2 cm, 5 μm, C18), and subsequently separated on an analytical column (Thermo Scientific EASY Column, 75 μm × 10 cm, 3 μm, C18) at a flow rate of 250 nL/min. The gradient program was as follows: solvent B was increased linearly from 0% to 35% over 0–50 min, from 35% to 100% over 50–58 min, and then maintained at 100% from 58 to 60 min.

After chromatographic separation, the samples were analyzed using a Thermo Scientific Q Exactive mass spectrometer. The total analysis time was 60 min. Data were acquired in positive ion mode with a full MS scan range of m/z 300–1800. The resolution for MS1 was set to 70,000 at m/z 200. The automatic gain control (AGC) target was 3×10^6, and the maximum injection time (Maximum IT) was 10 ms. The dynamic exclusion duration was set to 40.0 s. Peptide precursors and their fragment ions were acquired using a data-dependent acquisition (DDA) method. After each full scan (MS1), the top 10 most intense precursor ions were selected for MS/MS (MS2) analysis. The MS2 activation type

was higher-energy collisional dissociation (HCD), with an isolation window of 2 m/z. The MS2 resolution was set to 17,500 at m/z 200. The normalized collision energy (NCE) was 30 eV, and the underfill ratio was 0.1%.

2.14. Sequence database searching and data analysis

The MASCOT engine 2.2 (Matrix Science, London, UK) embedded into the Proteome Discoverer 1.4 Thermo Electron, San Jose, CA, USA was used to search the MS/MS spectra against the UniProt *Oryctolagus cuniculus* database (43,512 sequences, downloaded on November 11, 2021) and decoy databases. For protein identification, the following options were: peptide mass tolerance = 20 ppm; MS/MS tolerance = 0.1 Da; enzyme = trypsin; missed cleavage = 2; fixed modification: Carbamidomethyl (C), TMT16 (K), and TMT16 (N-term); variable modification: Oxidation (M). A decoy database strategy was applied for false discovery rate (FDR) estimation, and proteins were identified using an FDR threshold of $\leq$0.01. The protein ratios are calculated as the median of only unique peptides of the protein.

2.15. Bioinformatics analysis

Differentially expressed proteins were identified using the criteria of a fold change greater than 1.2-fold (an increase of more than 1.2-fold or a decrease of less than 0.83-fold) and a *p*-value of less than 0.05; the results are presented in a volcano plot. The hierarchical clustering algorithm performs cluster analysis on differentially expressed proteins from the comparison groups and presents the data in the form of a heatmap. The Gene Ontology (GO) program Blast 2 GO (https://www.blast2go.com/) and the Kyoto Encyclopedia of Genes and Genomes (KEGG) (http://www.genome.jp/kaas-bin/kaas_main) were used to annotate the differentially expressed proteins (DEPs) and bioinformatics analysis. GO was used to create histograms of GO annotations, including cell component, biological process, and molecular function. KEGG was used for pathway analysis.

Principal component analysis (PCA) was performed by linearly combining of protein expression data, extracting the constituent principal components, and visualizing the data in the form of score plots. In this study, the original data was imported into R language, where the ropls package was used for PCA analysis. Then, the data was normalized to UV, and the ggplot2 package was used for visualization. Protein–protein interaction (PPI) networks were constructed using the publicly available program STRING (http://string-db.org/), with the minimum required interaction score set at 0.400. The STRING is a database of known and predicted PPIs. PPIs included direct (physical) and indirect (functional) associations and were derived from four sources, i.e., genomic context, high-throughput experiments, coexpression, and previous knowledge.

2.16. Enzyme-linked immunosorbent assay (ELISA)

ELISA kits were used to measure the levels of ghrelin, dopamine (DA) (MM-82511O2, Meimian, Jiangsu, China), and 5-hydroxytryptamine (5-HT) (MM-37203O2, Meimian, Jiangsu, China) in the serum and the contents of lecithin, adenosine triphosphate (ATP) (MM-36796O2, Meimian, Jiangsu, China), ATP synthase (ATPase) (MM-82714O2, Meimian, Jiangsu, China), nicotinamide adenine dinucleotide (NADH) (MM-82717O2, Meimian, Jiangsu, China), cytochrome C (CytC) (MM-82719O2, Meimian, Jiangsu, China), CytC oxidase (COX) (MM-82725O2, Meimian, Jiangsu, China), and CytC reductase (CCR) (MM-82723O2, Meimian, Jiangsu, China) reductase in the hind leg muscle. The experimental procedures were conducted strictly in accordance with the protocol, with six biological replicates per group and three technical replicates per biological replicate.

2.17. Western blotting

Total protein of muscle samples was extracted with RIPA Lysis buffer (P0013B, Beyotime, Shanghai, China). Protein concentration was determined using a BCA kit (P0010S, Beyotime, Shanghai, China). Western blot was performed by using an appropriate dilution of the primary and secondary antibodies listed in Table S2. Glyceraldehyde-3-phosphate dehydrogenase (GAPDH) (Bioworld, Bloomington, MN, USA) was used as an internal control. The procedure is as follows: Equal amounts of protein (30 μg per sample) were separated by SDS-PAGE on an 8–12% polyacrylamide gel and then transferred to a PVDF membrane. After washing and blocking the PVDF membrane, it was incubated overnight at 4 °C with the primary antibody. After overnight incubation, the PVDF membrane was washed and incubated with the secondary antibody for 1 h at room temperature. Finally, the Chemiluminescence Imaging system (Monad, Wuhan, China) was used to scan the polyvinylidene fluoride (PVDF) membranes. The relative expression of the target protein was normalized by GAPDH. The same set of four biological replicates used for TMT proteomics analysis was also used for Western blot validation, with two technical replicates performed. All values were presented as mean ± SEM.

2.18. Statistical analysis

Imported data into the cloud platform (https://www.genescloud.cn/chart/chartOverview) for Spearman correlation analysis ($|r| > 0.6$, $p < 0.05$). Statistical analysis was performed using the SPSS 27.0 software. The Image-Pro Plus 6.0 software was used for the quantitative analysis of images. The GraphPad Prism 8.0 software was used for mapping. Results were presented as mean ± SEM. Prior to statistical analysis, the assumptions of normality and homogeneity of variance were assessed using the Shapiro–Wilk test and F test, respectively. When the data satisfied the assumptions of normal distribution and equal variances, differences among multiple groups were analyzed using one-way analysis of variance (ANOVA). When a significant main effect was detected, post hoc multiple comparisons were performed using Tukey's multiple comparison test. A value of $p < 0.05$ was considered statistically significant. An independent samples *t*-test was used to identify differentially expressed proteins between the two groups. Fisher's exact test was performed for GO functional enrichment analysis, and a $p < 0.05$ was considered statistically significant.

3. Results

3.1. Growth performance evaluation of rabbits

As shown in Fig. 1A, an experiment was designed to measure the effects of coprophagy prevention on the growth performance of New Zealand white rabbits. The daily feed intake of each rabbit was recorded during the whole experimental period. Our results indicated no difference in food intake among the three groups (Fig. 1B). Compared with the CON and sham-coprophagy prevention groups, the final body weight of rabbits in the coprophagy prevention group was significantly decreased (Fig. 1C, $p < 0.05$). The higher levels of ghrelin in the rabbits of the coprophagy prevention group suggested a higher appetite (Fig. 1D). However, the average daily gain of rabbits in the coprophagy prevention group was significantly lower than that in the other two groups (Fig. 1E, $p < 0.05$). As a result, the FCR was significantly increased by coprophagy prevention (Fig. 1F, $p < 0.01$). Furthermore, histological staining results indicated that the density of muscle fiber was increased by the coprophagy prevention treatment (Fig. 1G), and oil red O staining results showed that lipid droplet accumulation in the rabbit meat of the coprophagy prevention group increased significantly (Fig. 1H, $p < 0.001$). Together, these results indicated that coprophagy prevention treatment affected the growth performance and muscle morphology in rabbits.

3.2. 3.2 Meat quality evaluation of rabbits

The meat quality-related parameters of rabbits were evaluated after treatment with coprophagy prevention (Fig. 2). Meat color and pH values at 45 min and 24 h after slaughter were measured. Significant differences in meat color (i.e., a^* and b^* values) and pH at 45 min after slaughter among three groups were observed (Fig. 2A). a^* of the The meat quality-related parameters of rabbits were evaluated after treatment with coprophagy prevention group remained significantly higher than the other two groups after 24 h (Fig. 2B, $p < 0.05$). Although cooking loss was not affected by The meat quality-related parameters of rabbits were evaluated after treatment with coprophagy prevention treatment (Fig. 2C, $p > 0.05$), the drip loss of the The meat quality-related parameters of rabbits were evaluated after treatment with coprophagy prevention group was significantly higher than that of the CON group (Fig. 2D, $p < 0.05$), and the coarse ash content of the The meat quality-related parameters of rabbits were evaluated after treatment with coprophagy prevention group was significantly lower than those of the CON and sham-coprophagy prevention groups (Fig. 2E, $p < 0.05$). Consistent with the Oil red O staining results of rabbit meat shown in Fig. 1H, the triglyceride content in the coprophagy prevention group increased significantly (Fig. 2F, $p < 0.05$). The shear force was also reduced by coprophagy prevention treatment (Fig. S1).

The fatty acid composition and content of rabbit meat were listed in

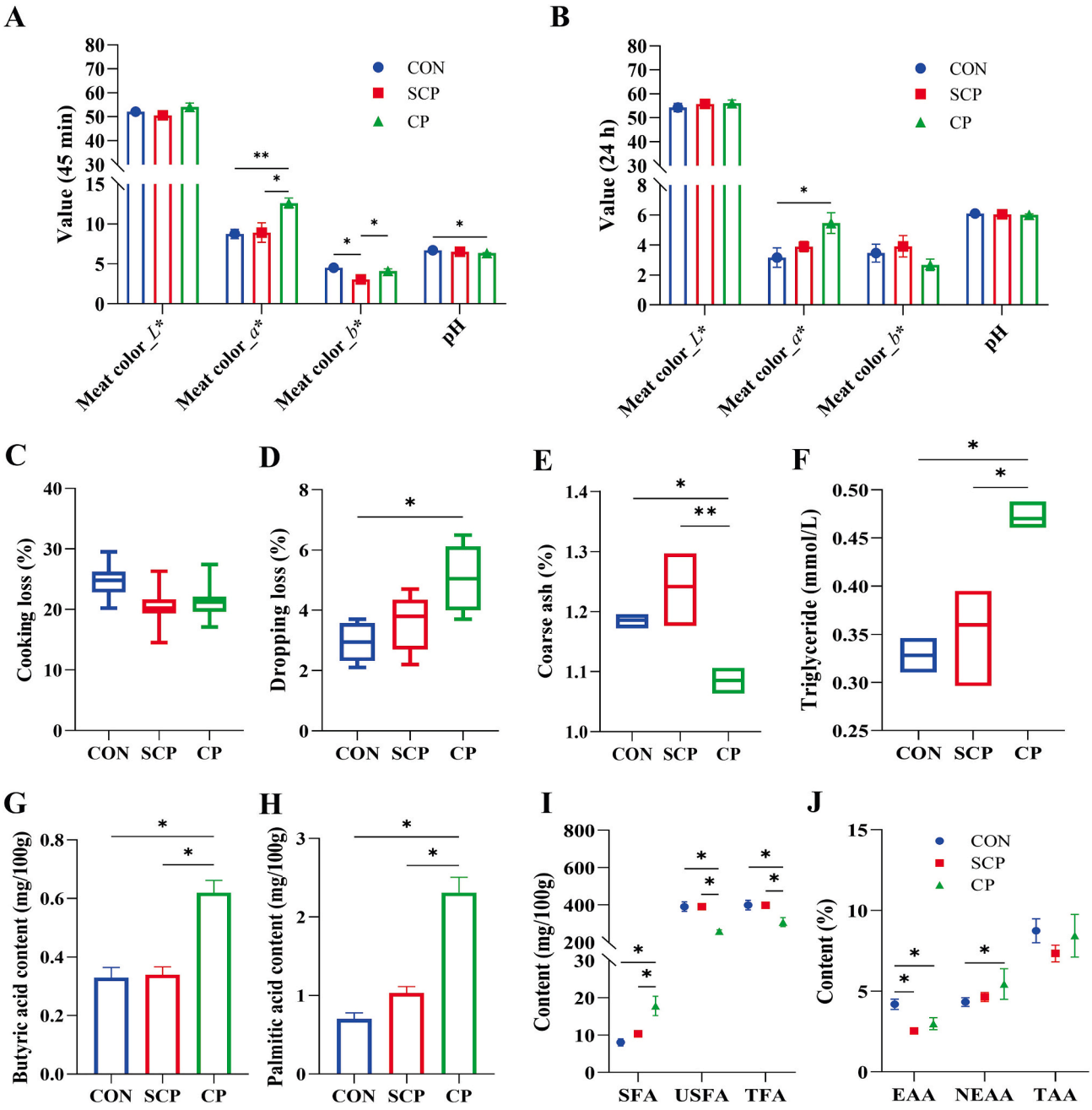

Fig. 2. Effects of CP on meat quality of rabbits. The color [lightness (L^*), redness (a^*), and yellowness (b^*)] and pH value at 45 min (A) and 24 h (B). The cooking loss (C), drip loss (D), coarse ash (E), triglyceride content (F), butyric acid content (G), palmitic acid content (H), fatty acid content (I) and amino acid content (J) of rabbit meat. SFA = saturated fatty acid, USFA = unsaturated fatty acid, TFA = total fatty acid, EAA = essential amino acid, NEAA = nonessential amino acid, TAA = total amino acid. CON = control, SCP = sham-coprophagy prevention, CP = coprophagy prevention; n = 6. Values are presented as mean ± SEM. The asterisks symbol indicates significant differences (*$0.01 < p \leq 0.05$, **$0.001 < p \leq 0.01$).

Table S3. Compared with the CON and sham-coprophagy prevention groups, the contents of butyric acid (Fig. 2G) and palmitic acid (PA, Fig. 2H) in the hind leg muscle of the coprophagy prevention group increased significantly ($p < 0.05$). Coprophagy prevention treatment caused a drastic increase in the content of saturated fatty acids (SFAs) and a significant decrease in the content of unsaturated fatty acids (USFAs; Fig. 2I, $p < 0.05$). The content and composition of amino acids were listed in Table S4. Our results suggested that coprophagy prevention treatment resulted in a remarkable decrease of EAAs while increase the content of nonessential amino acids (NEAAs; Fig. 2J, $p < 0.05$). In addition, the content of lecithin in rabbit meat increased under coprophagy prevention treatment (Fig. S2). Collectively, these results suggested that coprophagy prevention treatment had a negative influence on the meat quality of rabbits.

3.3. TMT quantitative proteomic analysis

TMT proteomics was performed to undertake an in-depth investigation and reveal the molecular mechanism of coprophagy prevention on meat quality and composition in rabbits. The heat map (Fig. 3A) showed a good overlap among muscle samples of three different treatments, PCA map (Fig. 3B) and the number of DEPs (fold change >1.2 or < 0.83 and p value <0.05, Fig. 3C) were listed in Fig. 3. In particular, the PCA plot revealed a clear separation between the coprophagy prevention group and both the CON and sham-coprophagy prevention groups. Moreover, the greater dispersion observed within the coprophagy prevention group suggests that the effects of coprophagy prevention treatment may vary among individuals. As shown in Fig. 3D, the Spearman correlation analysis of DEPs with meat quality-related parameters and nutritional compositions was performed. These correlations may initially reflect potential associations between DEPs and meat quality traits. Our results revealed that the a^* (45 min) value was positively correlated with myosin-7 (MYH7), NADH: ubiquinone oxidoreductase subunit (NDUFAB1), fatty acid binding protein 3 (FABP3), malate dehydrogenase 1 (MDH1), AB1acetyl-CoA acetyltransferase 1 (ACAT1), acyl carrier protein, and NAD(P)H quinone dehydrogenase 1 (NQO1) (r = 0.74, 0.76, 0.81, 0.76, 0.86, and 0.83, respectively; p = 0.04, 0.03, 0.01, 0.03, 0.01, and 0.01, respectively). However, the a^* (45 min) values was negatively correlated with the expression of myosin-4 (MYH4), CytC oxidase subunit 7A1 (COX7A1), and holocytochrome c-type synthase (HCCS) (r = −0.76, −0.98, and −0.90, respectively; p = 0.03, < 0.01, and < 0.01, respectively). Notably, drip loss was positively correlated with MYH7, FABP3, apolipoprotein A-I (APOA1), and NQO1 (r = 0.76, 0.81, 0.83, and 0.79, respectively; p = 0.03, 0.01, 0.01, and 0.02, respectively). Cooking loss was negatively correlated with FABP3, MDH1, ACAT1, and NQO1 (r = −0.79, −0.74, −0.86, and − 0.83, respectively; p = 0.02, 0.04, < 0.01, and 0.01, respectively). The contents of triglyceride and SFAs (especially butyric acid and PA) were positively correlated with MYH7 (r = 0.81 and 0.79, respectively; p = 0.01 and 0.02, respectively), FABP3(r = 0.81 and 0.93,

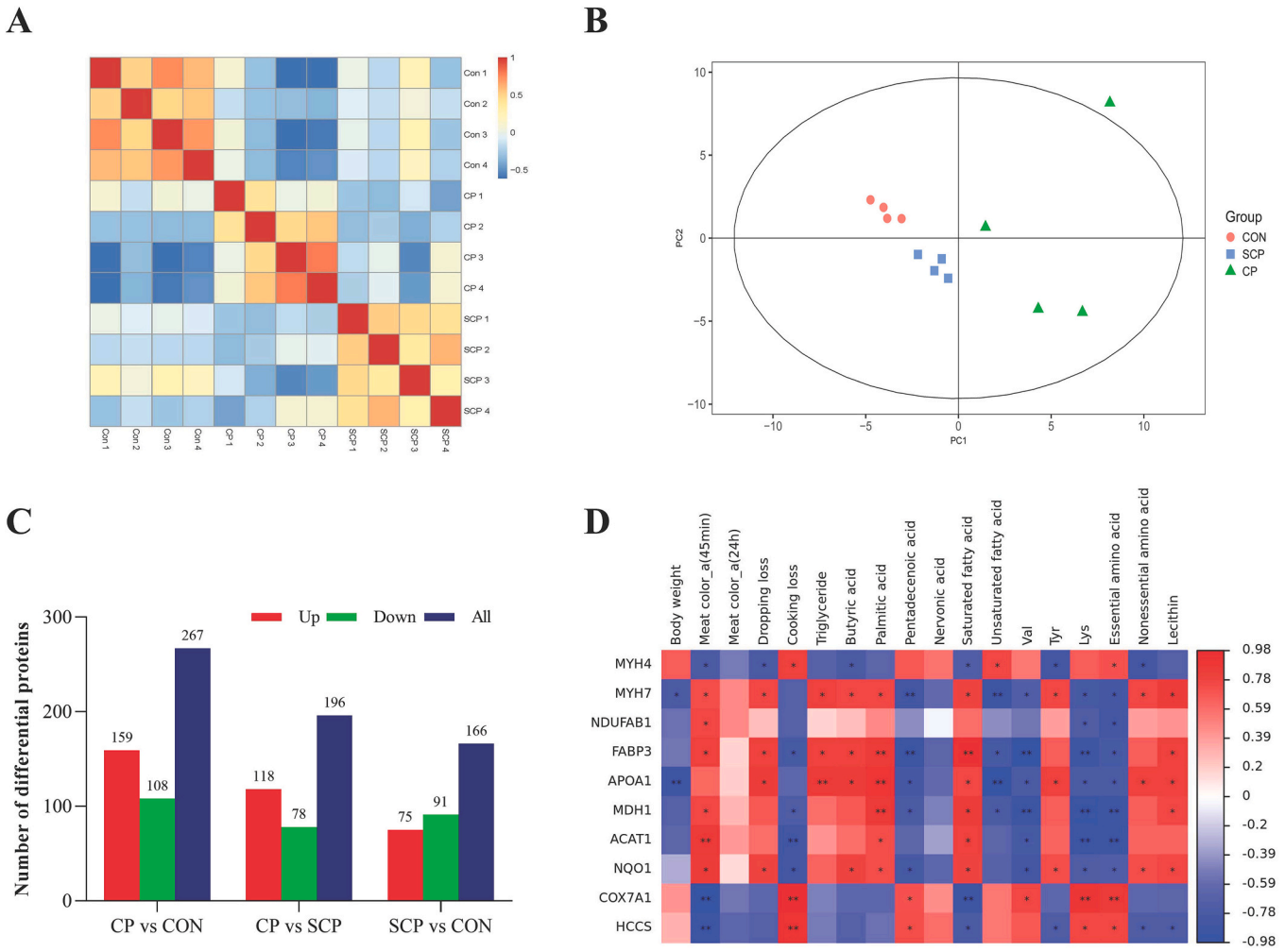

Fig. 3. TMT proteomics sequencing. (A) Heat map of correlation between samples. (B) Principal component analysis (PCA). (C) Number of DEPs. (D) Spearman correlation analysis between the DEPs and meat quality-related parameters and compositions. CON = control, SCP = sham-coprophagy prevention, CP = coprophagy prevention; n = 4. The asterisks symbol indicates significant differences (*0.01 < $p \leq$ 0.05, **0.001 < $p \leq$ 0.01).

respectively; $p = 0.01$ and < 0.01, respectively), and APOA1 ($r = 0.86$ and 0.76, respectively; $p = 0.01$ and 0.03, respectively). Pentadecenoic acid (USFA) and Lys (EAA) were positively correlated with COX7A1 ($r =$ 0.71 and 0.88, respectively; $p = 0.05$ and < 0.01, respectively) and HCCS (r = 0.74 and 0.76, respectively; $p = 0.04$ and 0.02, respectively). Moreover, pentadecenoic acid (USFA) and EAAs (i.e., Val and Lys) were negatively correlated with MYH7 ($r = -0.86$ and -0.81, respectively; $p = 0.01$ and $= 0.01$, respectively), FABP3 ($r = -0.90$ and -0.79, respectively; $p < 0.01$ and $= 0.02$, respectively), APOA1 ($r = -0.81$ and -0.76, respectively; $p = 0.01$ and $= 0.03$, respectively), MDH1(r = -0.76 and -0.88, respectively; $p = 0.03$ and < 0.01, respectively), and NQO1(r = -0.79 and -0.71, respectively; $p = 0.02$ and 0.05, respectively).

Based on the volcano plots (Fig. 4A) and hierarchical cluster analysis (Fig. 4B) of DEPs, 267 proteins were differentially abundant between CON and coprophagy prevention groups. The coprophagy prevention group had 159 up-regulated proteins and 108 down-regulated proteins relative to the CON group. Details of DEPs among these three treatments are listed in Supplementary File 2. Hierarchical clustering analysis indicated good reproducibility and high similarity of protein expression profiles among biological replicates within each group (Fig. 4B).

3.4. Bioinformatics analysis of DEPs

GO enrichment and KEGG pathway analyses were performed to identify the functional terms of DEPs. A total of 267 proteins were categorized by molecular functions, cellular components, and biological processes (Fig. 4C). For the molecular functions of DEPs between CON and coprophagy prevention groups, binding proteins (such as actin filament binding, tubulin binding, potassium ion binding, oxygen binding) were mostly enriched, and the phosphatase activity and structural constituent of extracellular matrix were also involved. The major cellular components affected by coprophagy prevention were myofibrils (including Z disc, basement membrane, and myosin complex) relative to the CON group. The most significantly enriched biological processes were involved in the process of transportation (including mitochondrial electron transport, CytC to oxygen, protein import into nucleus, and muscle tissue morphogenesis). The biological pathways associated with the identified DEPs by using the KEGG pathway analysis are shown in Fig. 4D. The most significant pathway terms included oxidative phosphorylation, non-alcoholic fatty liver disease, Parkinson's disease, muscle contraction, carbon metabolism, and pyruvate metabolism signaling pathways. PPI networks were constructed to investigate the interactions of these DEPs by coprophagy prevention (Fig. 4E). The top cluster was enriched in calcium-, muscle growth-, development-, and contraction-related proteins, whereas the second cluster was neurocognitive and energy metabolism-related proteins. The third cluster was involved in fatty acid transport and lipid metabolism, and this cluster was interlinked between the top two clusters.

Furthermore, the analysis results of the sham-coprophagy prevention/coprophagy prevention group (Fig. S3 and Fig. S4) were similar to the CON/coprophagy prevention group. The most significant pathway terms included oxidative phosphorylation, fat digestion and absorption, and diabetic cardiomyopathy (Fig. S4B). Based on the combined results of the sham-coprophagy prevention/coprophagy prevention and CON/coprophagy prevention comparisons, we suggest that oxidative phosphorylation may represent a key pathway associated with lipid deposition in the skeletal muscle of the coprophagy prevention group.

3.5. Verification of TMT quantitative proteomics analysis

To validate the reliability of the results obtained TMT quantitative proteomics analysis, especially for the metabolic pathways of cognition, skeletal muscle energy metabolism, oxidative phosphorylation, and lipid metabolism, validation experiments were carried out. Our findings indicated that the concentration of serum DA and 5-HT in rabbits of the coprophagy prevention group was significantly lower relative to those of the CON group (Fig. 5A, $p < 0.05$). Moreover, compared with those of CON and sham-coprophagy prevention groups, oxidative phosphorylation (Fig. 5C) and energy metabolism (Fig. 5B) in the skeletal muscle of the coprophagy prevention group were markedly decreased. However, the lipid synthesis and accumulation processes were activated in the coprophagy prevention group. This is evidenced by the significant increase in the expression of key proteins involved in lipid synthesis, such as CEBPA, PPARG, and Acrp 30 (Fig. 5D, $p < 0.05$). In summary, the impact of coprophagy prevention treatment on the total lipid content and fatty acid profiles was likely attributed to alterations in the oxidative phosphorylation and lipid synthesis pathways. A schematic model was drawn to summarize our research findings (Fig. 6).

4. Discussion

Studies focusing on the behavior of coprophagy of different species including horses (Ralston, 1986), dogs (Hart et al., 2018), voles (Kenagy & Hoyt, 1979), and rabbits (Li, Li, et al., 2020), have attracted increasing attention in recent years. Coprophagy is closely associated with nutrition intake (Savage, 1986), microflora implantation (Hu et al., 2021), chemical metabolism (Watarai et al., 2018), neural cognition (Bo et al., 2020), and other metabolic pathways. Regarding coprophagy in rodents (such as mice, voles, etc.), previous research has primarily focused on aspects such as energy metabolism, digestion and absorption, as well as gut microbiota (Cranford & Johnson, 1989; Ohta et al., 1996; Sha et al., 2023; Sukemori et al., 2003). Many rodents, along with rabbits, are typical laboratory and model animals. However, distinct from rodents, rabbits also possess unique economic attributes, with their fur and carcass holding significant economic value. Based on unique economic characteristics of rabbits, this study selected New Zealand white rabbits to investigate the effects of coprophagy prevention on muscle metabolism, meat quality, and the underlying molecular mechanism.

First, we evaluated whether the coprophagy prevention model affected normal feed intake in rabbits by recording daily feed intake and subsequently measuring serum ghrelin levels. We found that during the first four days, both the sham-coprophagy prevention and coprophagy prevention groups exhibited reduced feed intake due to stress caused by the collars. However, after an adaptation period, no significant effect of the collars on feed intake was observed. Moreover, the serum ghrelin results further supported this conclusion. During the initial stage of the experiment, only mild and transient discomfort associated with collar wearing was observed. After the adaptation period, no obvious signs of persistent distress or injury were detected. In the subsequent experimental period, no significant body weight loss, sustained anorexia, or severe distress was observed among the three groups of rabbits, except for an effect on grooming behavior, which was attributable to the physical restriction imposed by the collars.

Under efficient production systems, rabbits exhibit a high efficiency of protein utilization, converting approximately 20% of dietary protein into meat, which is only slightly lower than that of poultry (22–23%) (Kumar et al., 2025). Rabbit meat contains approximately 67–75% moisture and about 22% protein, which is consistent with our findings (Dalle Zotte & Szendrő, 2011). Drip loss and cooking loss are key indicators of muscle water-holding capacity and are therefore closely associated with meat texture and tenderness. In the present study, the increased drip loss observed in the leg muscle of the coprophagy prevention group indicates a reduced water-holding capacity. This may lead to decreased product yield during subsequent meat storage and processing (due to increased loss of intrinsic water and weakened water retention capacity), thereby adversely affecting meat quality to some extent. Rabbit meat is a highly nutritious functional food, and regular consumption may help control cardiovascular and other chronic diseases, partly due to its high content of polyunsaturated fatty acids (Dalle Zotte & Szendrő, 2011). It is characterized by high protein content, low cholesterol levels, and a greater proportion of essential amino acids.

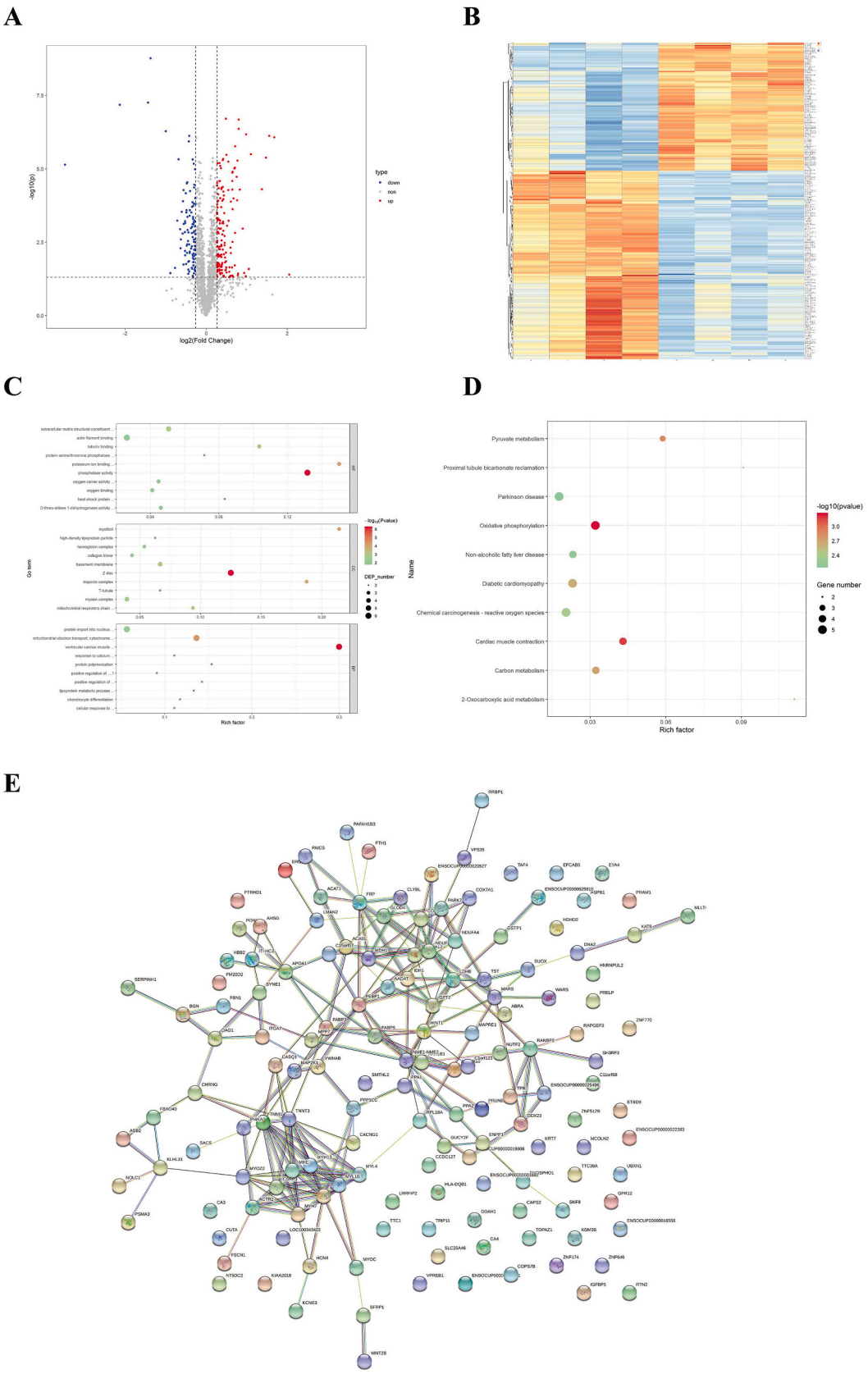

Fig. 4. Comparison, enrichment analysis and PPI network of DEPs affected by CP. (A) Volcano plot of the CON/CP group. (B) Hierarchical clustering analysis of the DEPs between CON and CP group (Blue, red and white indicate decrease, increase and no detectable changes in the expression abundance of DEPs, respectively). Go (C) and KEGG (D) functional annotation classification of the DEPs in CON/CP group. (E) PPI network of the total differentially expressed proteins of rabbit under CP treatment. PPI: protein-protein interaction. CON = control, SCP = sham-coprophagy prevention, CP = coprophagy prevention; n = 4. (For interpretation of the references to color in this figure legend, the reader is referred to the web version of this article.)

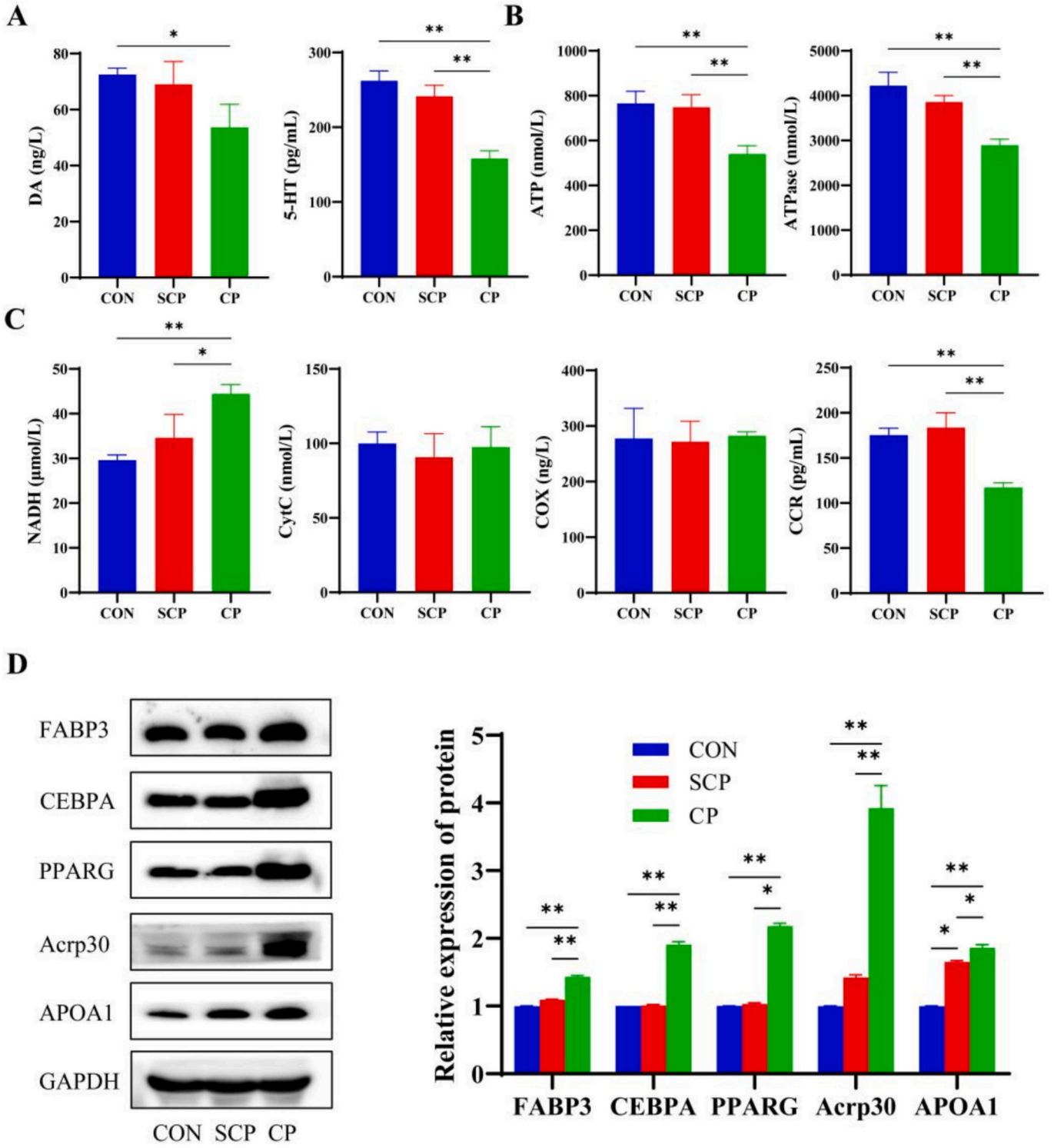

Fig. 5. Verification of TMT quantitative proteomics analysis. Effects of CP on neurocognitive ability (A), ATP production (B), oxidative phosphorylation (C) and expression of lipid accumulation-related proteins (D). CON = control, SCP = sham-coprophagy prevention, CP = coprophagy prevention; Fig. A-C, n = 6; Fig. D, n = 4. Values are presented as mean ± SEM. The asterisks symbol indicates significant differences (*$0.01 < p \leq 0.05$, **$0.001 < p \leq 0.01$).

Compared with other meats, rabbit meat is particularly rich in essential amino acids such as lysine, sulphur-containing amino acids, threonine, valine, isoleucine, leucine and phenylalanine; it is therefore a healthy choice of meat (Chen et al., 2021; Hernandez & Dalle Zotte, 2010). This high and balanced content of essential amino acids confers rabbit meat with significant nutritional value. Adequate intake of amino acids, particularly EAAs, which cannot be synthesized by the body and must be obtained from the diet, is crucial (Wang et al., 2025). However, coprophagy prevention processing reduces the levels of essential amino acids in leg muscles (primarily leucine, phenylalanine, and valine), thereby diminishing their nutritional value to some extent. From the perspective of fatty acid composition, coprophagy prevention treatment leads to a significant increase in saturated fatty acids, which is inconsistent with consumers' expectations for healthier dietary.

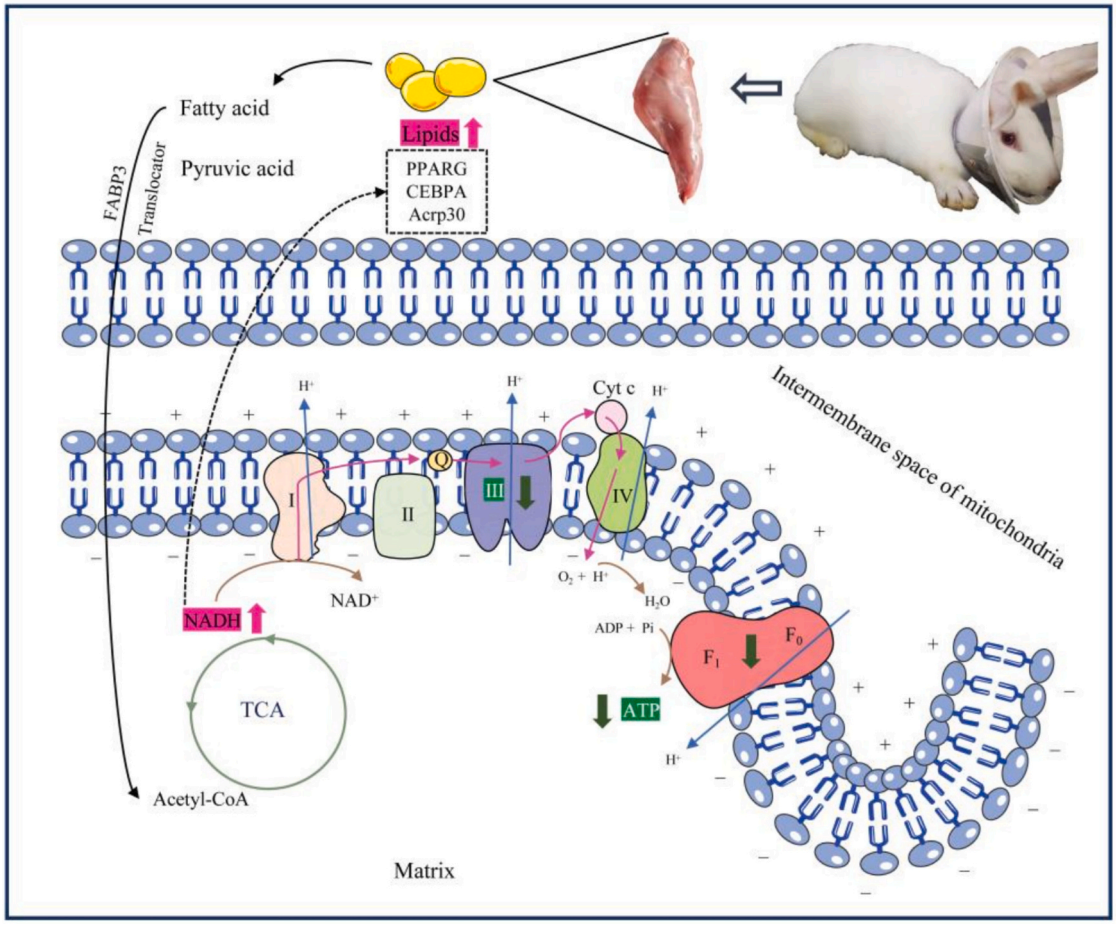

Fig. 6. Schematic model summarizing the regulatory mechanism of CP on lipid synthesis and accumulation in rabbit.

Fat content and fatty acid composition are important economical traits that are closely related to the flavor and nutritional value of meat. However, lipid synthesis and accumulation metabolism are regulated and affected by multiple factors (Li, Feng, & He, 2020). According to our previous studies, coprophagy prevention treatment significantly altered the gut microbiota of rabbits and reduced the levels of SCFAs in the caecum contents (Li, Li, et al., 2020; Wang et al., 2023). However, whether the declines in growth performance and meat quality observed in the present study are caused by changes in the gut microbiota and their metabolites remains unclear. Many other studies showed that gut microbiota is important for maintaining the metabolic health and elicit disease (Fan & Pedersen, 2021; Wang & Zhao, 2018), and changes in the gut microbiota are reported to be involved in lipid metabolism (Schoeler & Caesar, 2019). This finding is also evidenced by our previous study describing that coprophagy plays an important role in fat intake (Wang et al., 2019). Previous studies have shown that supplementation with probiotics can improve growth performance and meat quality in rabbits (Elbaz et al., 2025). SCFAs, as metabolites of the gut microbiota, have potential regulatory effects on muscle development and metabolism, and may influence meat quality through the "gut–muscle" axis (Liu et al., 2026; Malhi et al., 2025; Morrison & Preston, 2016). Previous studies have shown that supplementing rabbit diets with sodium butyrate can improve meat quality (Ni et al., 2025). Based on this, we hypothesize that the declines in growth performance and meat quality are at least partially attributed to gut microbiota changes after coprophagy prevention treatment, and further research is needed.

Currently, proteomics technology has been playing a pivotal role in studying biological systems and identifying disease-related proteins (Rozanova et al., 2021). It is also a powerful post-genomic tool that has been widely applied in meat science research to elucidate the complex biological mechanisms underlying meat quality traits (Jia et al., 2021). Quantitative proteomics has been utilized to assess the meat quality of beef and duck (He et al., 2019; Rodríguez-Vázquez et al., 2020). Among the identified differential proteins, MYH4 and MYH7 are involved in determining muscle composition and influencing contraction–relaxation activity in skeletal muscles (Ahn et al., 2018). Research has demonstrated that APOA1 is the main apolipoprotein of high-density lipoprotein, which is crucial for lipid metabolism and cholesterol transportation (Larsen et al., 2021). MDH1, NQO1, COX7A1, and HCCS are enzymes involved in energy metabolism. Our results suggested that coprophagy prevention induced an inhibition of oxidative phosphorylation, ATP synthesis, and energy metabolism (lipid metabolism) in rabbits. In previous studies, ATP synthesis reduction caused by oxidative phosphorylation inhibition is proved to be associated with the pathogenesis of a myriad of diseases spanning all organ systems (Nolfi-Donegan et al., 2020). Neutral lipid fatty acids stored in lipid droplets are absorbed into the mitochondria to produce ATP by oxidative phosphorylation (Bradley & Swann, 2019). Other studies also showed that changes in the concentration of NADH (substrate of the electron transport chain in oxidative phosphorylation) is a reflection of fat content (Wilson, 2017). Therefore, we hypothesize that the inhibition of mitochondrial oxidative phosphorylation caused by coprophagy prevention contributes to abnormal lipid accumulation. Our further verification results also revealed an increase in NADH content and a decrease in complex III (CytC reductase), ATP synthase, and ATP concentration. Finally, these changes may increase lipid accumulation. In addition, our study suggested a significant increase in the content of PA and the expression of transporter protein (FABP3) in the coprophagy prevention group and

that PA is widely reported to be an inducer of lipid metabolism dysfunction (Dong et al., 2020; Frampton et al., 2020). These findings provide a basis for further investigation into the molecular regulatory mechanisms underlying abnormal lipid accumulation induced by coprophagy prevention. This study also suggested a significant increase in the lecithin level of the coprophagy prevention group. Lecithin is widely accepted to promote lipid oxidation and reduce lipid accumulation (Shen et al., 2021). Thus, the increase in lecithin may be a compensatory mechanism caused by abnormal lipid accumulation.

Several limitations should be acknowledged in the present study. Although a sham-coprophagy prevention group was included for comparison, the potential influence of the collar itself cannot be completely excluded, particularly in the absence of behavioural assessments. In addition, although inhibition of oxidative phosphorylation was proposed as a potential mechanism underlying lipid deposition induced by coprophagy prevention, this hypothesis was not further supported by in-depth functional validation. Furthermore, our hypothesis that coprophagy prevention affects rabbit meat quality was partly based on previously reported alterations in gut microbial structure and hepatic lipid deposition. However, direct associations among gut microbiota, microbial metabolites, and meat quality traits were not established in the current study, and therefore the proposed mechanistic link remains speculative. Several limitations are also associated with the proteomics analysis. The selection of four samples per group based on proximity to the group mean was originally intended to minimise the influence of outliers; however, we recognise that this approach was not truly random and may have introduced selection bias, potentially underestimating intra-group variability while exaggerating inter-group differences. In addition, no correction for multiple testing was applied during differential protein expression analysis, which may increase the risk of false-positive findings. Although molecular validation was performed for pathways related to oxidative phosphorylation and lipid synthesis, the remaining proteomic findings should still be interpreted with caution. Accordingly, the proteomic results of the present study should be considered exploratory and hypothesis-generating rather than confirmatory. Future studies using larger sample sizes, independent randomly sampled cohorts, behavioural assessments, and integrated microbiome–metabolome analyses are needed to further validate and extend the present findings.

5. Conclusion

Our research suggests that coprophagy prevention is associated with impaired growth performance and altered meat quality in rabbits, as reflected by reductions in several meat-related parameters and nutritional constituents, together with an increased FCR. In addition, coprophagy prevention was associated with reduced serum dopamine DA and 5-HT levels, although the functional significance of these changes remains unclear in the absence of behavioural assessments. Proteomic profiling identified differentially expressed proteins mainly enriched in pathways related to muscle development, energy metabolism, fatty acid transport, and lipid metabolism. Further analyses suggested that the increased lipid accumulation observed in rabbit meat may be associated with alterations in mitochondrial oxidative phosphorylation and ATP production; however, these potential mechanistic relationships require further validation. Fig. 6 summarizes the main findings of the present study. Overall, these findings provide preliminary insights into the biological significance of coprophagy and its potential associations with growth performance and meat quality in rabbits. Further studies integrating behavioural evaluation and functional validation are needed to clarify the underlying mechanisms involved.

CRediT authorship contribution statement

Hui He: Writing – review & editing, Writing – original draft, Methodology, Data curation. **Zhitong Wang:** Validation, Software, Methodology, Data curation. **Zhichao Li:** Software, Methodology, Data curation. **Mengke Ni:** Validation, Methodology, Conceptualization. **Mengjuan Chen:** Methodology, Data curation. **Chaohui Guo:** Methodology. **Yaping Wang:** Validation, Software. **Hanfang Cai:** Writing – review & editing. **Ming Li:** Supervision, Methodology, Conceptualization. **Huifen Xu:** Writing – review & editing, Methodology.

Declaration of competing interest

The authors declare that they have no known competing financial interests or personal relationships that could have appeared to influence the work reported in this paper.

Acknowledgments

This research was jointly supported by the “National Key Research and Development Program of China (2018YFD0502203)”, “Special Fund for Henan Agriculture Research System (HARS-22-13-G1)” and “Special Fund for the Construction of National Modern Agricultural Industrial Park of Biyang County (NMAIP-BY-S01)”.

Appendix A. Supplementary data

Supplementary data to this article can be found online at https://doi.org/10.1016/j.fochms.2026.100421.

Data availability

Data will be made available on request.

References

Ahn, J. S., Kim, D.-H., Park, H.-B., Han, S.-H., Hwang, S., Cho, I.-C., & Lee, J.-W. (2018). Ectopic overexpression of porcine Myh1 increased in slow muscle fibers and enhanced endurance exercise in transgenic mice. *International Journal of Molecular Sciences, 19*(10), E2959. https://doi.org/10.3390/ijms19102959

Bo, T.-B., Zhang, X.-Y., Kohl, K. D., Wen, J., Tian, S.-J., & Wang, D.-H. (2020). Coprophagy prevention alters microbiome, metabolism, neurochemistry, and cognitive behavior in a small mammal. *The ISME Journal, 14*(10), 2625–2645. https://doi.org/10.1038/s41396-020-0711-6

Bradley, J., & Swann, K. (2019). Mitochondria and lipid metabolism in mammalian oocytes and early embryos. *The International Journal of Developmental Biology, 63*(3–4–5), 93–103. https://doi.org/10.1387/ijdb.180355ks

Burger-van Paassen, N., Vincent, A., Puiman, P. J., van der Sluis, M., Bouma, J., Boehm, G., … Renes, I. B. (2009). The regulation of intestinal mucin MUC2 expression by short-chain fatty acids: Implications for epithelial protection. *The Biochemical Journal, 420*(2), 211–219. https://doi.org/10.1042/BJ20082222

Chen, J., Yu, X., Huang, W., Wang, C., & He, Q. (2021). A novel angiotensin-converting enzyme inhibitory peptide from rabbit meat protein hydrolysate: Identification, molecular mechanism, and antihypertensive effect in vivo. *Food & Function, 12*(23), 12077–12086. https://doi.org/10.1039/D1FO02830H

Combes, S., Gidenne, T., Cauquil, L., Bouchez, O., & Fortun-Lamothe, L. (2014). Coprophagous behavior of rabbit pups affects implantation of cecal microbiota and health status. *Journal of Animal Science, 92*(2), 652–665. https://doi.org/10.2527/jas.2013-6394

Cranford, J. A., & Johnson, E. O. (1989). Effects of Coprophagy and diet quality on two microtine rodents (Microtus pennsylvanicus and Microtus pinetorum). *Journal of Mammalogy, 70*(3), 494–502. https://doi.org/10.2307/1381421

Dalle Zotte, A., & Szendrő, Z. (2011). The role of rabbit meat as functional food. *Meat Science, 88*(3), 319–331. https://doi.org/10.1016/j.meatsci.2011.02.017

Dong, Z., Xie, X., Sun, Y., Wu, H., & Dai, M. (2020). Paeonol prevents lipid metabolism dysfunction in palmitic acid-induced HepG2 injury through promoting SIRT1-FoxO1-ATG14-dependent autophagy. *European Journal of Pharmacology, 880*, Article 173145. https://doi.org/10.1016/j.ejphar.2020.173145

Ebino, K. Y. (1993). Studies on coprophagy in experimental animals. *Jikken Dobutsu. Experimental Animals, 42*(1), 1–9. https://doi.org/10.1538/expanim1978.42.1_1

Elbaz, N., Ashour, E. A., Bassiony, S. S., Elsherbeni, A. I., Mahgoub, S. A., Osman, A. O., … Abd El-Hack, M. E. (2025). Dietary probiotic supplementation with *Lactococcus lactis* and *Bacillus velezensis* enhances growth performance, meat quality, blood profiles, and cecal and feed microbiota in growing rabbits. *Animal Biotechnology, 36*(1), Article 2577947. https://doi.org/10.1080/10495398.2025.2577947

Fan, Y., & Pedersen, O. (2021). Gut microbiota in human metabolic health and disease. *Nature Reviews. Microbiology, 19*(1), 55–71. https://doi.org/10.1038/s41579-020-0433-9

Frampton, J., Murphy, K. G., Frost, G., & Chambers, E. S. (2020). Short-chain fatty acids as potential regulators of skeletal muscle metabolism and function. *Nature Metabolism, 2*(9), 840–848. https://doi.org/10.1038/s42255-020-0188-7

Hart, B. L., Hart, L. A., Thigpen, A. P., Tran, A., & Bain, M. J. (2018). The paradox of canine conspecific coprophagy. *Veterinary Medicine and Science, 4*(2), 106–114. https://doi.org/10.1002/vms3.92

Hays, K. E., Pfaffinger, J. M., & Ryznar, R. (2024). The interplay between gut microbiota, short-chain fatty acids, and implications for host health and disease. *Gut Microbes, 16*(1), 2393270. https://doi.org/10.1080/19490976.2024.239327

He, J., Xia, C., He, Y., Pan, D., Cao, J., Sun, Y., & Zeng, X. (2019). Proteomic responses to oxidative damage in meat from ducks exposed to heat stress. *Food Chemistry, 295*, 129–137. https://doi.org/10.1016/j.foodchem.2019.05.073

Hernandez, P., & Dalle Zotte, A. (2010). *Influence of diet on rabbit meat quality. In nutrition of the rabbit* (2nd edition, pp. 163–178). https://doi.org/10.1079/9781845936693.0163

Hopkins, D. L., & Thompson, J. M. (2001). The relationship between tenderness, proteolysis, muscle contraction and dissociation of actomyosin. *Meat Science, 57*(1), 1–12. https://doi.org/10.1016/S0309-1740(00)00065-6

Hu, X., Wang, F., Yang, S., Yuan, X., Yang, T., Zhou, Y., & Li, Y. (2021). Rabbit microbiota across the whole body revealed by 16S rRNA gene amplicon sequencing. *BMC Microbiology, 21*(1), 312. https://doi.org/10.1186/s12866-021-02377-x

Huo, W., Weng, K., Gu, T., Luo, X., Zhang, Y., Zhang, Y., Xu, Q., & Chen, G. (2021). Effects of integrated rice-duck farming system on duck carcass traits, meat quality, amino acid, and fatty acid composition. *Poultry Science, 100*(6), Article 101107. https://doi.org/10.1016/j.psj.2021.101107

Jia, W., Shi, Q., Zhang, R., Shi, L., & Chu, X. (2021). Unraveling proteome changes of irradiated goat meat and its relationship to off-flavor analyzed by high-throughput proteomics analysis. *Food Chemistry, 337*, Article 127806. https://doi.org/10.1016/j.foodchem.2020.127806

Jin, S., Pang, Q., Yang, H., Diao, X., Shan, A., & Feng, X. (2021). Effects of dietary resveratrol supplementation on the chemical composition, oxidative stability and meat quality of ducks (Anas platyrhynchos). *Food Chemistry, 363*, Article 130263. https://doi.org/10.1016/j.foodchem.2021.130263

Kenagy, G. J., & Hoyt, D. F. (1979). Reingestion of feces in rodents and its daily rhythmicity. *Oecologia, 44*(3), 403–409. https://doi.org/10.1007/BF00545245

Kokoszyński, D., Piwczyński, D., Arpášová, H., Hrnčar, C., Saleh, M., & Wasilewski, R. (2019). A comparative study of carcass characteristics and meat quality in genetic resources Pekin ducks and commercial crossbreds. *Asian-Australasian Journal of Animal Sciences*, 1753–1762. https://doi.org/10.5713/ajas.18.0790

Koyun, O. Y., Callaway, T. R., Nisbet, D. J., & Anderson, R. C. (2022). Innovative treatments enhancing the functionality of gut microbiota to improve quality and microbiological safety of foods of animal origin. *Annual Review of Food Science and Technology, 13*, 433–461. https://doi.org/10.1146/annurev-food-100121-050244

Kumar, P., Sharma, N., Narnoliya, L. K., Verma, A. K., Umaraw, P., Mehta, N., … Sazili, A. Q. (2025). Improving quality and consumer acceptance of rabbit meat: Prospects and challenges. *Meat Science, 219*, Article 109660. https://doi.org/10.1016/j.meatsci.2024.109660

Larsen, A. H., Johansen, N. T., Gajhede, M., Arleth, L., & Midtgaard, S. R. (2021). Lipid-bound ApoE3 self-assemble into elliptical disc-shaped particles. *Biochimica Et Biophysica Acta. Biomembranes, 1863*(1), Article 183495. https://doi.org/10.1016/j.bbamem.2020.183495

Li, H., Feng, Z., & He, M.-L. (2020). Lipid metabolism alteration contributes to and maintains the properties of cancer stem cells. *Theranostics, 10*(16), 7053–7069. https://doi.org/10.7150/thno.41388

Li, R., Li, X., Huang, T., Wang, Y., Xue, M., Sun, S., Yan, D., Song, G., Sun, G., & Li, M. (2020). Influence of cecotrophy on fat metabolism mediated by caecal microorganisms in New Zealand white rabbits. *Journal of Animal Physiology and Animal Nutrition, 104*(2), 749–757. https://doi.org/10.1111/jpn.13309

Li, S., Zeng, W., Li, R., Hoffman, L. C., He, Z., Sun, Q., & Li, H. (2018). Rabbit meat production and processing in China. *Meat Science, 145*, 320–328. https://doi.org/10.1016/j.meatsci.2018.06.037

Liao, J., Zhang, P., Yin, J., & Zhang, X. (2025). New insights into the effects of dietary amino acid composition on meat quality in pigs: A review. *Meat Science, 221*, Article 109721. https://doi.org/10.1016/j.meatsci.2024.109721

Liu, H., He, L., Ma, N., Tan, P., Tang, Q., Cai, K., Men, Z., Lu, Y., Hu, D., Zhao, J., Nie, C., Yu, S., Kang, Y., & Ma, X. (2026). Gut-muscle axis improves meat quality by regulating energy metabolism. *Meat Science, 235*, Article 110050. https://doi.org/10.1016/j.meatsci.2026.110050

Malhi, K. K., Chen, J., Wang, T.-H., Huang, M.-Y., Xing, K.-P., Xing, H.-B., … Li, J.-L. (2025). Dietary supplementation with blended essential oils improves meat quality of broilers through SCFA-mediated gut-muscle axis. *Poultry Science, 104*(12), Article 105911. https://doi.org/10.1016/j.psj.2025.105911

Morrison, D. J., & Preston, T. (2016). Formation of short chain fatty acids by the gut microbiota and their impact on human metabolism. *Gut Microbes, 7*(3), 189–200. https://doi.org/10.1080/19490976.2015.1134082

Ni, M., Wang, Z., Li, Z., Chen, M., He, H., Cai, H., Chen, Z., Li, M., & Xu, H. (2025). Dietary supplement of sodium butyrate improves the growth performance and intestinal health by targeting Wnt/β-catenin signaling pathway in rabbits. *Animal Research and One Health, 3*(4), 389–404. https://doi.org/10.1002/aro2.71

Nolfi-Donegan, D., Braganza, A., & Shiva, S. (2020). Mitochondrial electron transport chain: Oxidative phosphorylation, oxidant production, and methods of measurement. *Redox Biology, 37*, Article 101674. https://doi.org/10.1016/j.redox.2020.101674

Ohta, A., Baba, S., Ohtsuki, M., Taguchi, A., Adachi, T., & Hara, H. (1996). Prevention of coprophagy modifies magnesium absorption in rats fed with fructo-oligosaccharides. *British Journal of Nutrition, 75*(5), 775–784. https://doi.org/10.1079/BJN19960181

Ralston, S. L. (1986). Feeding behavior. *Veterinary Clinics of North America: Equine Practice, 2*(3), 609–621. https://doi.org/10.1016/s0749-0739(17)30709-5

Rodríguez-Vázquez, R., Mato, A., López-Pedrouso, M., Franco, D., Sentandreu, M. A., & Zapata, C. (2020). Measuring quantitative proteomic distance between Spanish beef breeds. *Food Chemistry, 315*, Article 126293. https://doi.org/10.1016/j.foodchem.2020.126293

Rozanova, S., Barkovits, K., Nikolov, M., Schmidt, C., Urlaub, H., & Marcus, K. (2021). *Quantitative mass spectrometry-based proteomics: An overview. Methods in Molecular Biology (Clifton, N.J.). 2228* pp. 85–116). https://doi.org/10.1007/978-1-0716-1024-4_8

Savage, D. C. (1986). Gastrointestinal microflora in mammalian nutrition. *Annual Review of Nutrition, 6*, 155–178. https://doi.org/10.1146/annurev.nu.06.070186.001103

Schoeler, M., & Caesar, R. (2019). Dietary lipids, gut microbiota and lipid metabolism. *Reviews in Endocrine & Metabolic Disorders, 20*(4), 461–472. https://doi.org/10.1007/s11154-019-09512-0

Sha, H., He, X., Yan, K., Li, J., Li, X., Xie, Y., Yang, Y., Deng, Y., Li, G., & Yang, J. (2023). Blocking coprophagy increases the levels of inflammation and depression in healthy mice as well as mice receiving fecal microbiota transplantation from disease model mice donors. *APMIS, 131*(7), 351–368. https://doi.org/10.1111/apm.13326

Shen, Y., Zhang, S., Zhao, X., & Shi, S. (2021). Evaluation of a lecithin supplementation on growth performance, meat quality, lipid metabolism, and cecum microbiota of broilers. *Animals, 11*(9), 9. https://doi.org/10.3390/ani11092537

Soave, O., & Brand, C. D. (1991). Coprophagy in animals: A review. *The Cornell Veterinarian, 81*(4), 357–364.

Souza Vilela, J., Alvarenga, T. I. R. C., Andrew, N. R., McPhee, M., Kolakshyapati, M., Hopkins, D. L., & Ruhnke, I. (2021). Technological quality, amino acid and fatty acid profile of broiler meat enhanced by dietary inclusion of black soldier fly larvae. *Foods (Basel, Switzerland), 10*(2), 2. https://doi.org/10.3390/foods10020297

Stoeva, M. K., Garcia-So, J., Justice, N., Myers, J., Tyagi, S., Nemchek, M., … Eid, J. (2021). Butyrate-producing human gut symbiont, clostridium butyricum, and its role in health and disease. *Gut Microbes, 13*(1), Article 1907272. https://doi.org/10.1080/19490976.2021.1907272

Sukemori, S., Ikeda, S., Kurihara, Y., & Ito, S. (2003). Amino acid, mineral and vitamin levels in hydrous faeces obtained from coprophagy-prevented rats. *Journal of Animal Physiology and Animal Nutrition, 87*(5–6), 213–220. https://doi.org/10.1046/j.1439-0396.2003.00415.x

Thacker, E. J., & Brandt, C. S. (1955). Coprophagy in the rabbit: One figure. *The Journal of Nutrition, 55*(3), 375–385. https://doi.org/10.1093/jn/55.3.375

Wang, Y., Xu, H., Sun, G., Xue, M., Sun, S., Huang, T., … Li, M. (2019). Transcriptome analysis of the effects of fasting Caecotrophy on hepatic lipid metabolism in New Zealand rabbits. *Animals, 9*(9), E648. https://doi.org/10.3390/ani9090648

Wang, Z., He, H., Chen, M., Ni, M., Yuan, D., Cai, H., Chen, Z., Li, M., & Xu, H. (2023). Impact of coprophagy prevention on the growth performance, serum biochemistry, and intestinal microbiome of rabbits. *BMC Microbiology, 23*(1), 125. https://doi.org/10.1186/s12866-023-02869-y

Wang, Z., Zhang, R., Du, G., Ni, M., He, H., Li, Z., … Xu, H. (2025). Effects of the welfare housing systems based on environmental enrichment on growth performance, meat quality, and intestinal health in rabbits. *The FASEB Journal, 39*(10), Article e70636. https://doi.org/10.1096/fj.202500042R

Wang, Z., & Zhao, Y. (2018). Gut microbiota derived metabolites in cardiovascular health and disease. *Protein & Cell, 9*(5), 416–431. https://doi.org/10.1007/s13238-018-0549-0

Watarai, A., Arai, N., Miyawaki, S., Okano, H., Miura, K., Mogi, K., & Kikusui, T. (2018). Responses to pup vocalizations in subordinate naked mole-rats are induced by estradiol ingested through coprophagy of queen's feces. *Proceedings of the National Academy of Sciences of the United States of America, 115*(37), 9264–9269. https://doi.org/10.1073/pnas.1720530115

Wilson, D. F. (2017). Oxidative phosphorylation: Regulation and role in cellular and tissue metabolism. *The Journal of Physiology, 595*(23), 7023–7038. https://doi.org/10.1113/JP273839

Wiśniewski, J. R., Zougman, A., Nagaraj, N., & Mann, M. (2009). Universal sample preparation method for proteome analysis. *Nature Methods, 6*(5), 359–362. https://doi.org/10.1038/nmeth.1322

Zhao, Y.-L., Zhou, Y.-H., Chen, J.-Q., Huang, Q.-Y., Han, Q., Liu, B., … Li, Y.-H. (2015). Quantitative proteomic analysis of sub-MIC erythromycin inhibiting biofilm formation of S. Suis in vitro. *Journal of Proteomics, 116*, 1–14. https://doi.org/10.1016/j.jprot.2014.12.019

Zhou, H., Yu, Z., & Ye, Z. (2018). Key proteins associated to coloured compounds of peach peel using iTRAQ proteomic techniques during development and postharvest. *Scientia Horticulturae, 239*, 123–132. https://doi.org/10.1016/j.scienta.2018.05.036

Zhu, M., Liu, J., Xiao, J., Yang, L., Cai, M., Shen, H., Chen, X., Ma, Y., Hu, S., Wang, Z., Hong, A., Li, Y., Sun, Y., & Wang, X. (2017). Lnc-mg is a long non-coding RNA that promotes myogenesis. *Nature Communications, 8*, Article 14718. https://doi.org/10.1038/ncomms14718